The local and non-local components of the local field potential in awake primate visual cortex

Timothy J. Gawne

Abstract The Local Field Potential (LFP) is the analog signal recorded from a microelectrode inserted into cortex, typically in the frequency band of approximately 1 to 200 Hz. Here visual stimuli were flashed on in the receptive fields of primary visual cortical neurons in awake behaving macaques, and both isolated single units (neurons) and the LFP signal were recorded from the same unipolar micro-electrode. The fall-off of single unit activity as a visual stimulus was moved from near the center to near the edge of the receptive field paralleled the fall-off of the stimulus-locked (evoked) LFP response. This suggests that the evoked LFP strongly reflects local neuronal activity. However, the evoked LFP could be significant even when the visual stimulus was completely outside the receptive field and the single unit response had fallen to zero, although this phenomenon was variable. Some of the non-local components of the LFP may be related to the slow distributed, or non-retinotopic, LFP signal previously observed in anesthetized animals. The induced (not time-locked to stimulus onset) component of the LFP showed significant increases only for stimuli within the receptive field of the single units. While the LFP primarily reflects local neuronal activity, it can also reflect neuronal activity at more distant sites, although these non-local components are typically more variable, slower, and weaker than the local components.

1 Introduction

The Local Field Potential (LFP) is the low-frequency analog electrical activity that is recorded from a microelec-trode in cortex. It provides complementary information to that of single- or multi-unit activity, and is widely thought to reflect, not spiking, but synaptic potentials from a large number of neurons (Mitzdorf 1985). However, it is still not known how "local" the LFP really is. Different studies have yielded widely varying results, with estimates of the spread of activity reflected in the LFP signal ranging from a few hundred microns (Berens et al. 2008; Engel et al. 1990; Katzner et al. 2009; Kruse and Eckhorn 1996; Liu and Newsome 2006; Xing et al. 2009) to several millimeters (Kreiman et al. 2006; Logothetis et al. 2001; Mitzdorf 1985) in extent across cortex, although these studies vary in stimulus condition and even what aspect of the LFP is considered (such as frequency band, or evoked vs. induced).

In contrast to those studies that have mostly explored the spread of the LFP with physical distance over the cortical surface, this study uses a functional definition where the spatial range of inputs in visual space that activate single visual cortical units is compared with the range that affects the LFP.

2 Methods

2.1 Electrophysiological recordings

Recordings were made from V1 in two awake macaques (one *Macaca mulatta* and one *Macaca fascicularis*). Using

Action Editor: Gaute T. Einevoll

T. J. Gawne (✉)
Department of Vision Sciences,
University of Alabama at Birmingham (UAB),
924 South 18th St.,
Birmingham, AL 35294, USA
e-mail: tgawne@gmail.com

standard sterile techniques, each monkey was anesthetized with isoflurane, and an 18 mm-diameter PEEK (Polyether-etherketone) plastic recording chamber was implanted over the dorsal posterior skull. High-strength plastic strips were also bolted to the skull with ceramic screws and connected to a head-fixation system.

After recovery, each animal was trained to fixate on a small white square on a computer monitor. Eye position was monitored with a video tracking system (ISCAN), and juice rewards given for maintaining fixation to within + −0.5° of the target square. The video display was run at a frame rate of 85 Hz, positioned 57 cm away from the eye, and was 39 cm wide and 27 cm tall. Single-unit recording was made through a 23 gauge guide tube that penetrated the dura and allowed parylene-insulated microelectrodes (Microprobe) with tip impedances of approximately 1.2 megohms to be introduced into V1 cortex in the calcarine fissure, using techniques matching a previous study in this lab (Gawne and Martin 2002). Position was checked both via stereotaxic coordinates and MRI imaging. Peripheral V1 was used because the larger receptive fields reduced the effects of small errors of eye fixation. Microelectrodes were advanced using an hydraulically-driven microdrive (Narishige MO95). The electrode signal was amplified with an A-M Systems 1801 amplifier, and digitized at 32 kHz. Final spike isolation was performed offline using a principal-components based technique (Abeles and Goldstein 1977). The LFP was recorded in a parallel channel, using a 2-pole high pass Butterworth filter with a cutoff of 1 Hz, and a 4-pole low pass Bessel filter with a cutoff of 200 Hz. The LFP signal was digitized with a 16 bit A/D and a sampling rate of 1 kHz. To avoid saturation the LFP signal was amplified 10 times less than the spike signal. The recordings were made in an electrically shielded room with the video monitor placed outside and separated from the main room with a plate of electrically conductive glass. Listening to the LFP channel evinced no audible 60 Hz hum, nor was there any obvious 60 or 85 Hz periodic signals on the oscilloscope display.

2.2 Stimulus configuration

The stimulus configuration is illustrated in Fig. 1. The stimuli used in these experiments were selected from the set of 2D black and white Walsh patterns. These patterns were luminance-balanced with the uniform gray background (6.96 cd/m^2). As illustrated in Fig. 1(b), for each of the 22 neurons a single Walsh pattern was selected that could elicit a strong response from two different locations within the Receptive Field (RF) , although one stimulus was presented near the center of the RF and the other was presented near the edge. The stimuli were then presented both separately and in combination. A similar stimulus
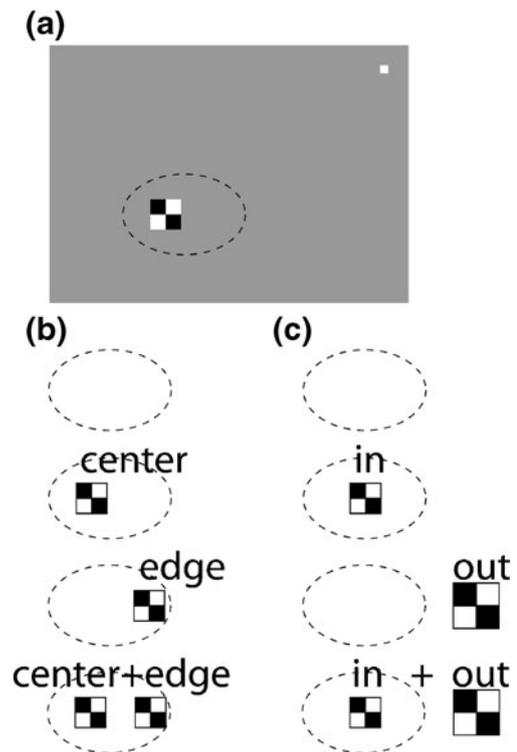

Fig. 1 Experimental design. (a) The monkeys fixated on a small white square, and the receptive fields were identified by hand mapping (figure not to scale). All stimuli had the same mean luminance as the uniform gray background. Stimuli were flashed on either singly or together in different locations within or outside of the RF. (b) Stimuli presented at different locations within the RF. There were four stimulus combinations: a null control, a single stimulus presented near the center of the RF ("center"), a single stimulus presented near the edge of the RF ("edge"), and both stimuli flashed on at the same time ("center+edge"). (c). Same as in panel (b), only here "in" is centered in the RF and "out" is located well outside the RF. In this case the stimulus outside the RF was three times the linear dimension of the stimulus inside the RF

presentation paradigm was used for 24 additional neurons, only in this case one stimulus was presented centered in the RF, and the other was presented well outside the RF (see Fig. 1(c)). In this latter case the stimulus presented outside the RF had a linear dimension three times that of the stimulus within the RF.

The receptive field centers ranged from 10.5 to 20.0° from the center of gaze, and the stimulus sizes varied from 0.4 to 1.0° in width. For the stimulus configuration illustrated in Fig. 1(b) the distance between the stimuli varied from 0.12 (nearly touching) to 1.5°. For the stimulus configuration presented in Fig. 1(c) the stimuli were separated by a range of 10 to 15°. There were four stimulus combinations: null stimulus, one stimulus by itself, the other stimulus by itself, and both stimuli together. These combinations were presented in shuffled random order, ideally 100 repetitions for each condition, minimally 30 repetitions, and with a median of 82 repetitions. Trials

where the animals did not maintain fixation were not included in these totals and were not analyzed. Rewards were given after every three or four stimulus presentations, and a three-second interval was inserted after the reward to minimize lick artifact in the LFP signal.

The stimuli were flashed on for 24 video frames at 85 Hz (approximately 282 msec duration), in a data acquisition window that lasted 440 msec. These 440 msec epochs were separated by intervals that varied randomly from 400 to 800 msec, except when a reward was given. Presenting the stimuli in short temporal epochs is consistent both with the brief duration of inter-saccadic intervals, and with the observed high speed of the visual system (Thorpe et al. 1996). Additionally, for most V1 cortical neurons the effects of flashing a stimulus on in the receptive field with the eyes fixed is comparable to having a saccade bring a constant stimulus into the receptive field (Gawne and Martin 2002; Richmond et al. 1999). Hence, this paradigm closely approximates the normal operating conditions of primate visual cortical neurons.

Any visual stimulus that an animal can perceive and respond to is a valid one. Walsh patterns are easy to generate on a video display, and they contain a broad spectrum of spatial frequencies which makes it relatively easy to elicit strong responses from visual cortical neurons in multiple visual areas. Careful analysis of the responses of visual cortical neurons has shown that the neuronal responses elicited by Walsh patterns have properties that are similar to the responses elicited by bars or naturalistic images (Weiner et al. 2001).

2.3 Data analysis

The single-unit responses were quantified by convolving the raw spike times with a Gaussian kernel with a σ= 3 msec, which has the effect of low-pass filtering with a cutoff frequency of 44 Hz. This creates a continuous spike density function (Silverman 1986), which is essentially a smoothed post-stimulus histogram, but with the advantage that it does not suffer from "bin-edge artifact" (the problem with histograms when changing spike times near the edge of two bins radically alters the appearance of the response).

The evoked components of the LFP were averaged time-locked to stimulus onset. The LFP signal was quite variable on a trial-by-trial basis (see Fig. 2(c)) and, unlike the case with action potentials, considerable averaging was required to get a reliable mean. This variability in the LFP signal is comparable to, although somewhat worse than, similar recordings in anesthetized macaques (see Xing et al. 2009 Figure 1G). Combined with the need to add a three-second post-reward timeout, this limited the total number of trials per recording site and meant that only paradigms with a

small number of unique conditions could be successfully completed.

For some recording sites there was a significant 85 Hz signal in the LFP that was time-locked to the video display, typically on the order of 15 μV peak-to-peak. This signal was not evident in any single trials, but only in the mean response. Therefore, the mean response as a function of time to a blank gray control stimulus was subtracted from the stimulus-evoked responses, which was effective in removing this interference. Peak LFP response was calculated as the difference between the maximum and minimum LFP during the analysis interval. Mean LFP was the mean of the absolute value of the LFP. Similar indices were also computed for the spiking response: peak spikes were the maximum of the spike density waveform during the analysis interval minus the peak during the null control stimulus, and mean spikes were the mean of the spike density function minus the mean during the null control stimulus.

The induced (non phase-locked to stimulus onset) LFP responses were also computed. First, the mean LFP response to a given stimulus condition was subtracted off from the LFP waveform for each individual trial. The resultant waveforms had a Hamming window applied to them, and then were padded with zeros to 2,000 points long to increase the apparent resolution in the lower frequency bands. The magnitude of the Fourier transform for the individual trials was averaged as a function of frequency. These induced components were generally weak and erratic, which prevented the application of more sophisticated techniques such as computing a time-frequency spectrogram. Instead, the mean value of the magnitude of the Fourier transform was computed in the alpha (8–12 Hz), beta (12–30 Hz), and gamma (30–100 Hz) bands across the entire duration of the response.

All experimental procedures and care of the animals were carried out in compliance with guidelines established by the National Institute of Health and were approved by the University of Alabama at Birmingham Animal Care and Use Committee.

3 Results

3.1 Stimuli near the center and the edge of the RF

Figure 2 shows an example of the spiking responses from one neuron and the LFP recorded simultaneously from the same unipolar microelectrode, using the paradigm illustrated in Fig. 1(b). The single-unit response (top and middle rows) shows that the response to the stimulus near the middle of the RF was relatively larger (leftmost panels), and the response to the less centrally located stimulus was
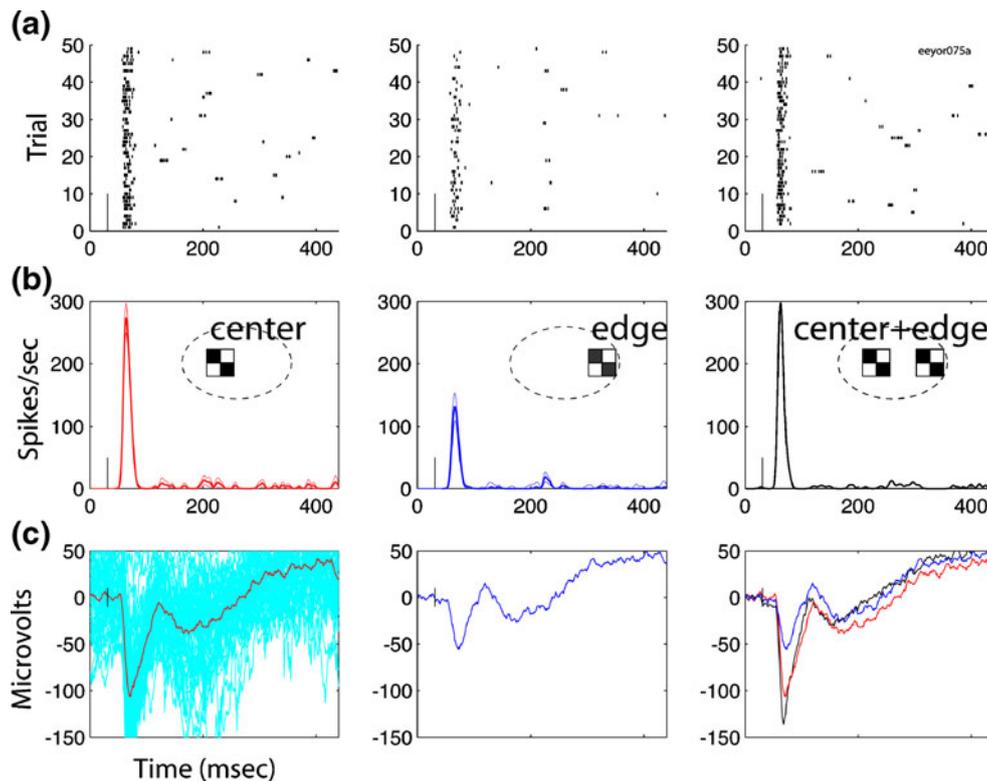
Fig. 2 Example of the responses of a single V1 cortical neuron to either a stimulus near the center of the RF (*leftmost column*) a stimulus near the edge of the RF (*middle column*), and both stimuli presented at the same time (*rightmost column*). Row (**a**) shows raster plots of single action potentials. Row (**b**) shows the corresponding mean spike-density waveform. Row (**c**) shows the evoked (stimulus-locked) component of the LFP. Stimulus onset is indicated by the vertical black bar at time = 31 msec. In the leftmost panel of row (**c**) the mean response is shown superimposed on the individual trials (*n*=64) illustrating the significant trial-by-trial variability of this signal. Note that both the single-unit response and the magnitude of the local field potential response are smaller for the conditions in the second column as compared to the first. When both stimuli are presented at the same time (*rightmost panels*) the single-unit response is almost identical to the single strongest response (*middle right panel*), but in this case the local field potential shows some additivity (*bottom right panel*)

relatively smaller (middle panels). The evoked component of the local field potential (bottom row) paralleled the single unit response, in that the single stimulus that elicited the strongest single-unit response also elicited the strongest LFP response. Changing the position of the stimuli within the RF changed only the magnitude of the LFP response, and did not affect the overall shape of the LFP waveform as a function of time. These results are typical of all neurons studied with this paradigm.

Figure 3 shows the correlation between the single unit and the evoked component of the LFP for 22 V1 neurons. The leftmost panels (a,b) illustrate the magnitude of the LFP response versus the magnitude of the single unit response. Plotted are the responses for the stimuli placed near the edge of the RF ("edge" from Fig. 1) normalized by the responses for the stimuli placed near the center of the RF ("center" from Fig. 1). Regardless of whether they are quantified as peak firing rate or as mean firing rate, the single unit response for the stimuli near the edge of the RF are always less than the responses for the stimuli near the middle of the RF, which is why these data are always in the left half-plane. When you move a stimulus away from the center of the RF you tend to decrease the LFP response the same proportional amount as the spiking response, which is why these data are clustered in the lower left quadrant rather than scattered uniformly over the entire left quadrant. However, looking at the interactions between two stimuli (panels (c) and (d)), we see little relationship between the LFP and spiking response. Thus, the data in Fig. 3 demonstrates that while the LFP response has the same falloff as the single unit response as a stimulus is moved out of the RF, the function that the LFP computes is not the same as the function computed by the locally-recorded neuron.

3.2 Stimuli inside and outside the RF

Figure 4(a) and (b) show the LFP and single-unit responses for one site where both the LFP and single-unit responses to a stimulus outside the RF were negligible. Figure 4(c) and (d) show an example from another recording site where the single-unit response was again exactly the same as the
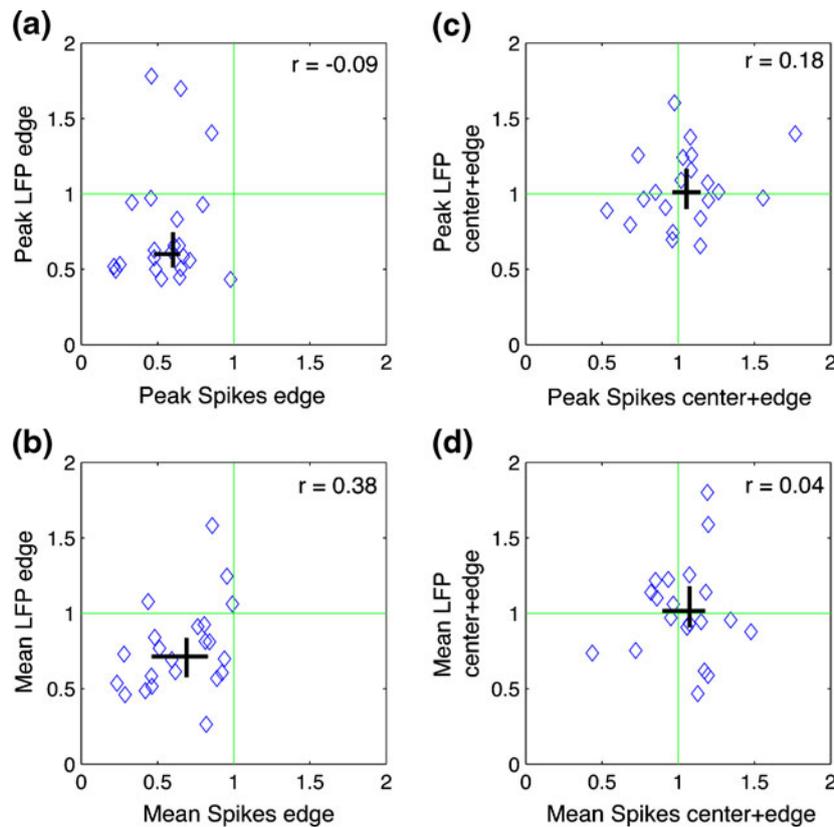
Fig. 3 Results for all recording sites for the stimulus paradigm illustrated in Fig. 1 panel (**b**). Panel (**a**) plots the peak LFP for the stimulus located near the edge of the RF (*vertical axis*) vs. the peak spike rate (*horizontal axis*). These values are normalized by the corresponding value for the stimulus that is presented nearer the center. Each point is the mean value for each of 22 neurons. The thick black horizontal and vertical lines are the bootstrapped 95% confidence intervals of the median of these points. Stimuli that elicit a smaller peak firing rate also elicit similarly smaller peak responses in the LFP (data clustered in lower left quadrant). Panel (**b**) is similar to panel (**a**), only this is a plot of the mean number of spikes versus the mean of the absolute value of the LFP over the same interval. As in panel (**a**), the stimuli placed near the edge of the RF tend to have both smaller spike counts and less integrated LFP activity. Panels (**c**) and (**d**) are similar in layout to panels (**a**) and (**b**), however, these are plots of the responses to both stimuli presented at the same time ("center +edge"), normalized by the response to the stimulus nearer the center of the RF ("center"). Overall, there is no relationship between the interactions of two stimuli between the spikes and the LFP

response to the null-control, but the LFP showed a relatively smaller but still definite response. In every case we found that the single unit response to the stimulus outside the RF was the same as the spontaneous activity, but the LFP response was variable.

Figure 5(a) illustrates examples from recording sites where there was a brief pulsatile component in the LFP response to a stimulus flashed outside the RF. The initial inflection point of this response varied from 15 to 38 msec longer than the initial inflection point of the response to a stimulus flashed inside the RF. There is also a slower, more gradual response, that peaks approximately 200 msec after stimulus onset, although this slow component was not always of the same polarity (note the negative polarity of the middle of the five traces). The difference between the "in+out" and "in" conditions is indicated by the gray lines ("Linear"). Despite the inherent difficulty in examining the small difference between two larger noisy signals, at least for some sites it does appear as if there is a tendency for the initial component to be compatible with linear summation. Figure 5(b) is the mean of the normalized LFP across all 24 recording sites. On average, the LFP responses to a stimulus inside the RF of a neuron are similar regardless of whether or not a stimulus is also present outside the RF. When a stimulus is present only outside the RF there is still an indication in the mean response of the brief pulsatile components seen in Fig. 5(a), and it appears to follow the linear prediction, that is, the trends along the waveform that is the difference between "in+out" and "in". The later broader component is more evident, but does not appear to follow the linear prediction.

To increase statistical power, the waveforms for each site for the "out" condition only were decomposed into two basis waveforms, labeled C1 and C2. C1 was chosen by hand to encompass the slower component, and was zero up to 90 msec after stimulus onset, +1 up until 270 msec after
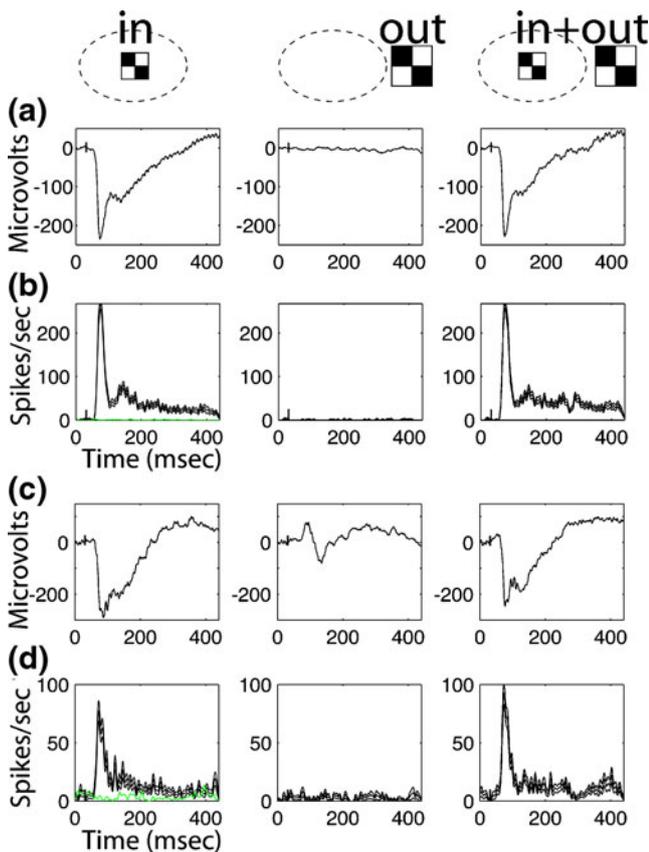
Fig. 4 Panel (a) shows the LFP responses and panel (b) the single unit responses from an example recording site where the stimuli were presented either centered in the RF (leftmost panels, "in") or outside the RF (middle panels, "out"). For this example neuron both the LFP and the single unit response went to zero for the stimuli outside the RF. Panels (c) and (d) are arranged similarly to panels (a) and (b), only for this site there was a small but definite LFP response to the stimulus outside the RF (see middle panel of panel (c), "in"). The spiking activity in the middle box of panel (d) was not different from the spontaneous activity, which is indicated at the bottom of the leftmost box of panel (d)

stimulus onset, and −1 until the end of the interval. C2 was everywhere zero except it was +1 in the interval from 31 to 62 msec after stimulus onset, and −1 from 63 to 94 msec. Both components were statistically different from zero (t-test, $P < 0.05$) and only weakly correlated, $r = 0.42$.

Figure 6 illustrates the induced (not time-locked to stimulus onset) LFP responses. These responses are much stronger in the lower than in the higher frequency bands. While induced peaks in the alpha-band were observed, no distinct stimulus-related peaks were observed at higher frequencies. Instead, the effect of a stimulus was simply a uniform increase in activity across a broad range of frequencies. Panels b,c, and d illustrate the activity in the alpha, beta, and gamma frequency bands averaging across the entire recording epoch and all 24 recording sites. There were statistically significant increases in the magnitude of the induced LFP in all three frequency bands for a single

stimulus presented inside the RF (t-test, $P < 0.05$). There appeared to be a trend for a stimulus outside the RF to decrease the induced activity below baseline, but this was not significant. There was not a statistically significant difference between the condition with a stimulus located inside the RF by itself, and paired with a stimulus located outside the RF (paired t-test, $P > 0.05$).

4 Discussion

The results presented here indicate that in awake behaving primates the LFP is generally dominated by local neuronal activity. In particular, the spatial range of visual stimuli that elicit significant single-unit activity is the same as that which generates strong LFP activity. This is in agreement with a recent study using combined microelectrode and optical recording that also found the LFP to be driven by local processing (Katzner et al. 2009), and another study in anesthetized macaques which found that the spread of the evoked LFP across the cortical surface matched the spread of the multi-unit activity to visual stimuli (Xing et al. 2009). However, although variable, the LFP can be significantly driven by stimuli that are far outside the RF. From estimates of the cortical magnification factor in rhesus monkeys (Gatass et al. 1981), visual stimuli of these eccentricities and separations should correspond to a distance on the surface of V1 of between approximately 2.2 to 3.3 mm.

Previous studies on anesthetized cats have found that there is a short-latency LFP component that matches the extent of the spike-defined RF, and a longer-latency LFP component that has a more broad spatial distribution. (Bringuier et al. 1999; Doty 1958; Ebersole and Kaplan 1981; Kitano et al. 1994, 1995; Kasamtsu et al. 2005; Mitzdorf 1985). This aspect of the LFP has variously been referred to as the "non-retinotopic" or "Slow Distributed Component" (SDC). The brief pulsatile non-local components of the LFP illustrated in Fig. 5(a) have a similar latency and form, and therefore may be related to these previously identified slow distributed components.

There are several possible mechanisms that could account for the non-local components of the LFP. They could be due to direct electrical volume conduction of signals from distant areas of cortex, or they could be due to local synaptic activity that is driven by distant neuronal activity, either through propagation via horizontal connections within cortex or through diffuse feedback connections from other cortical regions. Of course, in the intact awake animal all of these effects could be present in variable degrees depending upon the experimental conditions, and the use of anesthetized or brain-slice preparations could additionally change the balance of these effects.
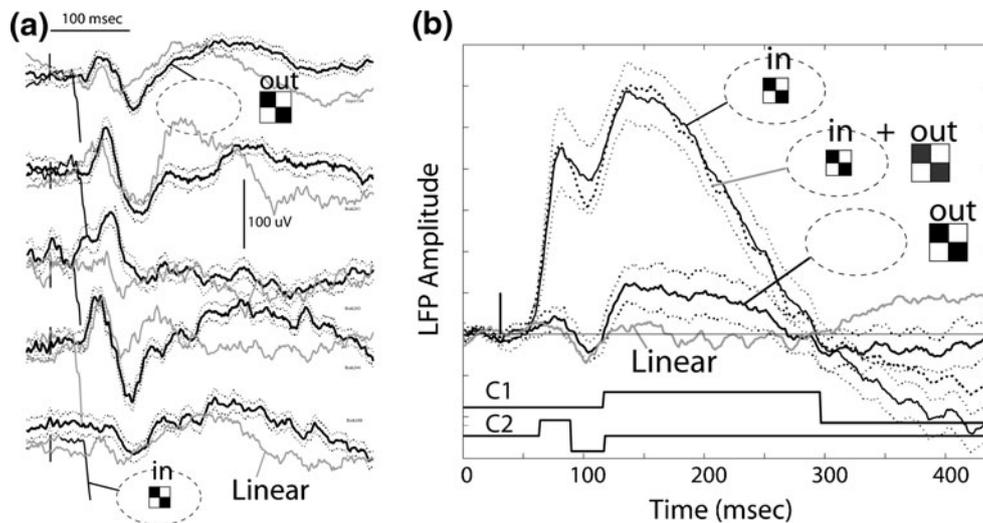
Fig. 5 Panel (**a**) illustrates examples of cases where there was a small transient LFP response to a stimulus outside the RF (*solid black lines*, *dashed lines* are the standard error of the mean from the individual trials, median *n*=82). The *thin black lines* are the truncated response to a stimulus flashed inside the RF, showing the earlier inflection point for this condition. Note also that there is a slower, more rounded response as well, but which was not of a constant polarity (see middle of the five example waveforms). The *gray line* labeled "Linear" is the difference between the response to a stimulus "out+in" minus the response to "in" only. Panel (**b**) illustrates the mean over all sites (*n*= 24) of the responses to a single stimulus inside the RF (*black line*, "in"), a stimulus both inside and outside the RF (*gray line*, "in+out"), and a stimulus only present outside the RF (*black line near the bottom*, "out"). These responses were first normalized by the peak of the response to a stimulus inside the RF only before averaging. The *dotted line at the bottom* is the mean across all sites of the difference between the in, and in+out conditions ("Linear"). If the LFP response to both stimuli was the linear sum of the responses to both stimuli presented separately, this curve should track the response to the stimulus presented outside the RF by itself. The two lines labeled "C1" and "C2" at the bottom represent the two components that the waveforms were decomposed into (see text)

The volume conduction of electrical signals in cortex should be essentially instantaneous. Additionally, at the frequency bands of interest cortical tissue does not have significant filtering effects (Logothetis et al. 2007), and so should not cause phase delays or otherwise cause any distortion or temporal dispersion of a signal. Therefore, it would seem that the longer-latency non-local component of the LFP cannot be due to volume conduction effects. However, this need not be the case. Consider that the latency of the skin-surface recorded VEP is typically much longer than the latency of visual cortical single unit responses (Fahle and Bach 2006). This difference in latency is clearly not due to delays caused by axonal conduction. Rather it appears to be caused by the distant volume-conducted potential being selective for patterns of activity that are coherent over large areas (a *spatial* low-pass filter), and which have longer stimulus-defined onset latencies than high *spatial* frequency patterns of activity (Nunez et al. 2001). Even as volume conduction can result in a significant evoked signal many millimeters or even centimeters away at the surface of the skin, it can surely also affect a microelectrode embedded within the cortex itself. Obviously, any volume-conducted signal would not be detectable with a bipolar recording electrode, and would be strongly affected by changes in local tissue geometry such as might occur with a non-conductive window placed over

cortex, or in isolated slice preparations. Finally, while the volume conduction of signals transmitted from different areas should exhibit perfect linear summation with local signals, there are conditions where this might not hold. In particular, if the slow distributed component were uniformly distributed across all of cortex, then it would be present and of the same magnitude regardless of condition, and linear summation with local signals would not be observed.

A non-local component of the LFP could also be caused by local synaptic activity driven either from diffuse feedback connections or spreading horizontal waves of activity within cortex. Demonstrating that stopping local synaptic activity eliminates the non-local component would be strong evidence for one of these possibilities (Kitano et al. 1994, 1995; Kasamtsu et al. 2005) although as these studies used a bipolar recording electrode one would not expect to pick up a distant volume-conducted signal. It should be noted that a steadily increasing latency as a stimulus is moved farther and farther away from the RF need not be evidence of horizontally spreading waves in cortex (see Bringuier et al. 1999). As mentioned previously, the farther one travels from an electrical source in the brain the more one will tend to be selective for patterns of activity that are coherent over progressively larger spatial scales, and which could be progressively slower or lower in frequency. Hence, even for the volume conduction of
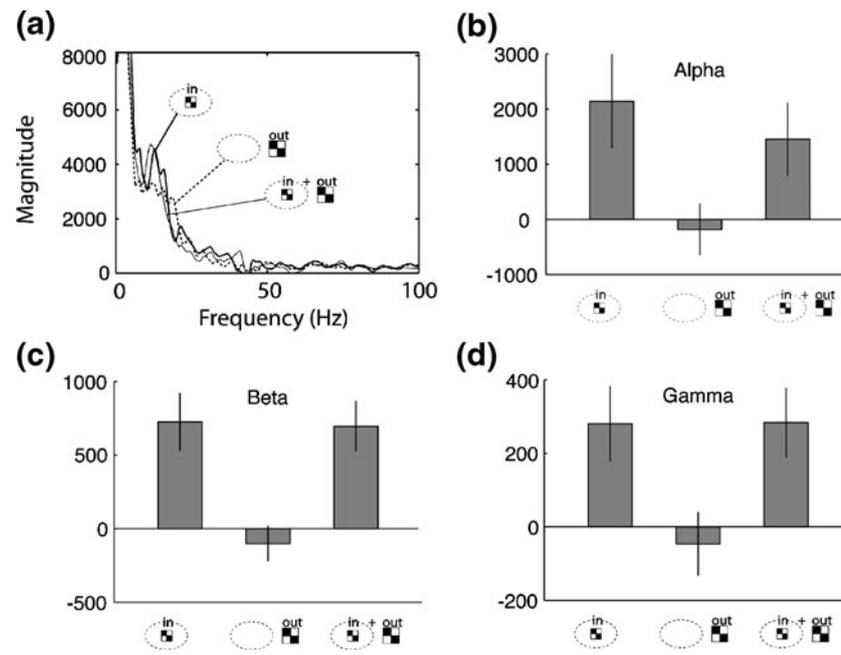
Fig. 6 Panel (**a**) illustrates the magnitude of the Fourier transform of the induced (not phase-locked to stimulus onset) component of the LFP for one example neuron. Spontaneous activity when a null stimulus was presented was subtracted off. The magnitude of the signal fell off rapidly with increasing frequency. (**b**) Mean value of the magnitude of the Fourier transform of the induced component of the LFP in the alpha band (8–12 Hz), $n=24$, error bars are the standard error of the mean. There is a significant increase in alpha-band power when a stimulus is flashed in the receptive field, but flashing a stimulus outside the RF has no significant effect regardless of whether or not it is paired with a stimulus inside the RF. Similar results were obtained in the beta (**c**) and gamma (**d**) frequency bands

distant signals, one might expect a steadily increasing latency with increasing distance. Conceivably a similar sort of result could be obtained with feedback from other cortical areas, if more broadly distributed feedback connections reflected activity from slower processes.

The brief pulsatile non-local LFP components would seem to be created by a different sort of process than the slower more rounded component, both because of differences in timing and because there is at least a trend for the former to be better fit by a linear-summation model than the latter. The slower component is unlikely to be due to visual stimulus-dependent eye movements, both because data with large eye movements during the recording epoch were edited out, and because the minimal latency between the presentation of a visual stimulus and an eye movement is at least 200 msec (Leigh and Zee 2006), to which must be added visual processing delays. It has been shown that the presentation of a visual stimulus with no net luminance can cause a pupillary reaction (Gamlin et al. 1998), but again, the pupillary response latency is on the order of 200 msec. It also seems unlikely that these LFP responses could be due to history effects, both because the inter-recording epoch was of variable duration, and because the baseline activity from the null stimulus was subtracted off. The slower non-local LFP component is typically not reported in anesthetized preparations, sug-

gesting that it represents some sort of diffuse cognitive or alerting signal.

The locality of the LFP signal has been explored by comparing the degree of tuning for a stimulus parameter (such as orientation) for both the LFP and single-unit activity (Katzner et al. 2009). Finding that both the LFP and single unit signal have similar orientation tuning does indeed indicate a strong local LFP component. However, when using stimuli that vary in orientation, any non-local effects would tend to average out to a uniform baseline because distant from the recording site there will be many locations that are activated by any given orientation, and the non-local signal would therefore be constant and lost in the baseline. Turning a single distant stimulus on and off, as was done in this study, is therefore more likely to uncover non-local effects.

5 Conclusion

In agreement with most previous studies, the results presented here confirm that the LFP is dominated by local neuronal activity. The induced LFP was only significant when there was local neuronal activity. However, in agreement with other studies using anesthetized animals, it has here been demonstrated in awake primates that there

can be a non-local component to the evoked LFP. Under the conditions of this study the non-local component was highly variable, and at some sites gave the appearance of the slow distributed component seen in anesthetized animals. It is hypothesized that the non-local component will be strongest when distant stimuli are large in area, synchronously turn on and off, and there is no local stimulus to mask the distant effects.

References

Abeles, M., & Goldstein, M. H., Jr. (1977). Multispike train analysis. *Proceedings of the IEEE, 65*, 762–773.

Berens, A., Keliris, G. A., Ecker, A. S., Logothetis, N. K., & Tolias, A. S. (2008). Comparing the feature selectivity of the gamma-band of the local field potential and the underlying spiking activity in primate visual cortex. *Frontiers in Systems Neuroscience, 2*, 1–11.

Bringuier, V., Chavane, F., Glaeser, L., & Frégnac, Y. (1999). Horizontal propagation of visual activity in the synaptic integration field of area 17 neurons. *Science, 283*, 695–699.

Doty, R. W. (1958). Potentials evoked in cat cerebral cortex by diffuse and by punctiform photic stimuli. *Journal of Neurophysiology, 21*, 437–464.

Ebersole, J. S., & Kaplan, B. J. (1981). Intracortical evoked potentials of cats elicited by punctate visual stimuli in receptive field peripheries. *Brain Research, 224*, 1601–1664.

Engel, A. K., König, P., Gray, C. M., & Singer, W. (1990). Stimulus-dependent neuronal oscillations in cat visual cortex: inter-columnar interaction as determined by cross-correlation analysis. *European Journal of Neuroscience, 2*, 588–606.

Fahle, M., & Bach, M. (2006). Origin of the visual evoked potentials. In J. R. Heckenlively & G. B. Arden (Eds.), *Principles and practice of clinical electrophysiology of vision* (2nd ed.). Cambridge: MIT.

Gamlin, P. D. R., Zhang, H., Harlow, A., & Barbur, J. L. (1998). Pupil responses to stimulus color, structure and light flux increments in the rhesus monkey. *Vision Research, 38*, 3353–3358.

Gattass, R., Gross, C. G., & Sandell, J. H. (1981). Visual topography of V2 in the macaque. *Journal of Comparative Neurology, 201*, 519–539.

Gawne, T. J., & Martin, J. M. (2002). Responses of primate visual cortical neurons to stimuli presented by flash, saccade, blink, and external darkening. *Journal of Neurophysiology, 88*, 2178–2186.

Kasamtsu, T., Mizobe, K., & Sutter, E. (2005). Muscimol and baclofen differentially suppress retinotopic and nonretinotopic responses in visual cortex. *Visual Neuroscience, 22*, 839–858.

Katzner, S., Nauhaus, I., Benucci, A., Bonin, V., Ringach, D. L., & Carandini, M. (2009). Local origin of field potentials in visual cortex. *Neuron, 61*, 35–41.

Kitano, M., Niiyama, K., Kasamatsu, T., Sutter, E. E., & Norcia, A. M. (1994). Retinotopic and nonretinotopic field potentials in cat visual cortex. *Visual Neuroscience, 11*, 953–977.

Kitano, M., Kasamatsu, T., Norcia, A. M., & Sutter, E. E. (1995). Spatially distributed responses induced by contrast reversal in cat visual cortex. *Experimental Brain Research, 104*, 279–309.

Kreiman, G., Hung, C. P., Kraskov, A., Quiroga, R. Q., Poggio, T., & DiCarlo, J. J. (2006). Object selectivity of local field potentials and spikes in the macaque inferior temporal cortex. *Neuron, 49*, 433–445.

Kruse, W., & Eckhorn, R. (1996). Inhibition of sustained gamma oscillations (35–80 Hz) by fast transient responses in cat visual cortex. *Proceedings of the National Academy of Science, 93*, 6112–6117.

Leigh, R. J., & Zee, D. S. (2006). *The neurology of eye movements* (4th ed.). Oxford: Oxford University Press.

Liu, J., & Newsome, W. T. (2006). Local field potential in cortical area MT. Stimulus tuning and behavioral considerations. *Journal of Neuroscience, 26*, 7779–7790.

Logothetis, N. K., Pauls, J., Augath, M., Trinath, T., & Oeltermann, A. (2001). Neurophysiological investigation of the basis of the fMRI signal. *Nature, 412*, 150–157.

Logothetis, N. K., Kayser, C., & Oeltermann, A. (2007). *In vivo* measurement of cortical impedance spectrum in monkeys: implications for signal propagation. *Neuron, 55*, 809–823.

Mitzdorf, U. (1985). Current source-density method and application in cat cerebral cortex: investigation of evoked potentials and EEG phenomena. *Physiological Reviews, 65*, 37–100.

Nunez, P. L., Wingeier, B. M., & Silberstein, R. B. (2001). Spatial-temporal structures of human alpha rhythms: theory, microcurrent sources, multiscale measurements, and global binding of local networks. *Human Brain Mapping, 13*, 125–164.

Richmond, B. J., Hertz, J. A., & Gawne, T. J. (1999). The relation between V1 neuronal responses and eye movement-like stimulus presentations. *Neurocomputing, 26–27*, 247–254.

Silverman, B. W. (1986). *Density estimation for statistics and data analysis*. New York: Chapman and Hall.

Thorpe, S., Fize, D., & Marlot, C. (1996). Speed of processing in the human visual system. *Nature, 381*, 520–521.

Weiner, M. C., Oram, M. W., Liu, Z., & Richmond, B. (2001). Consistency of encoding in monkey visual cortex. *Journal of Neuroscience, 21*, 8210–8221.

Xing, D., Yeh, C. I., & Shapley, R. M. (2009). Spatial spread of the local field potential and it laminar variation in visual cortex. *Journal of Neuroscience, 29*, 11540–11549.